Permeability and morphology study of polysulfone composite membrane blended with nanocrystalline cellulose

Haolong Bai, Xuan Wang, Haibo Sun, Liping Zhang*

College of Materials Science and Technology, Beijing Forestry University, No. 35 Qinghua East Road, Beijing 100083, China
Tel. +86 13911868160; email: zhanglp418@163.com

ABSTRACT

Polysulfone (PS) composite membranes blended with nanocrystalline cellulose (NCC) for ultrafiltration were prepared by a Loeb–Sourirajan phase inversion process. The effect of NCC content, PS content, and additive content on both permeability and morphology of composite membranes were studied. The surface and cross-section morphologies of the composite membranes were investigated using scanning electron microscopy with both the porosity and mean pore size of composite membranes being compared. The experimental result showed that the morphology of composite membranes changed significantly with the aforementioned factors. Through the experimental work, the proper composite membrane preparation condition was obtained as follows. The NCC content was 0.3 wt% and the PS content was 18 wt%. The solvent was N,N-dimethylacetamide. Polyethylene glycol 1000 was used as the additive with a concentration of 3 wt%. The coagulation bath was deionized water and its temperature was maintained at 30℃. Due to the addition of NCC the pure water flux of composite membrane increased from 175.6 L/(m²h) in the pure PS to 343.2 L/(m²h), the porosity and mean pore size of composite membrane increased from 40.5% and 33.6 nm in the pure PS membrane to 67.6%, 47.1 nm, respectively.

Keywords: Polysulfone (PS); Nanocrystalline cellulose (NCC); Membrane; Permeability; Morphology

1. Introduction

Ultrafiltration (UF) is a filtration process driven by pressure difference. Owing to its advantages such as ease of operation and low energy consumption, UF process has been widely applied in the domain of water treatment, wastewater treatment, desalination process, food processing industry, pharmacy industry and biotechnology, etc. [1–5].

Polysulfone (PS) is one of the most widely used UF membrane materials due to its features such as high mechanical property, good thermal, physical and chemical stability, etc. [6–8]. However, same as other types of hydrophobic membrane materials, the intrinsic hydrophobic property of PS causes membrane fouling problems in its application in UF, resulting in a sharp decrease of the membrane permeability. Consequently, many researchers have carried out hydrophilic modification on membranes including physical blending, chemical grafting, surface

*Corresponding author.

modifying, etc. [9,10]. Comparatively speaking, physical blending is advantageous in an easy preparation with the use of phase inversion [9]. With the rapid development of nanotechnology, the blending of nanoparticles with membrane materials is attracting more and more attention. It is well known that nanoparticles, with small size, huge specific surface area, and strong activity, have unique magnetic, electronic, mechanical, and optical properties which could improve the properties of polymers to a certain extent [11,12]. It is reported that some inorganic nanoparticles, such as nano Al_2O_3 particles [13] and nano TiO_2 particles [14] have been used to enhance hydrophilicity and other properties of the membrane.

It is well known that cellulose is an environmentally friendly biopolymer and an almost inexhaustible and sustainable polymeric raw material [15]. Nanocrystalline cellulose (NCC) not only retains the characteristics of natural cellulose such as biodegradability, renewability, and hydrophilicity, but also has the features of nanoparticles including huge specific surface area, high mechanical strength, and tensile modulus [16,17]. NCC can be produced by either chemical or mechanical treatment. The chemical method, such as strong acid hydrolysis, removes the amorphous regions of cellulose fiber and produces nanoscale fibrils [18]. The mechanical method involves a high-pressure homogenizer treatment [19], a grinder treatment [20,21], and a high-pressure refiner treatment [22]. Compared with inorganic nanoparticles, NCC with a high axis (L/D) has gained more attention owing to its easy availability, renewability, and low density [23,24]. In general, cellulose fibrils in nanoscale are very popular for polymer reinforcement and hydrophilicity enhancement in composite materials preparation [25].

In this paper, NCC was prepared with the combination of chemical and mechanical treatment from the raw material cellulose pulp. After the process of acid hydrolysis, the cellulose pulp was homogenized by a high-pressure homogenizer in order to reduce the hydrolysis acid concentration while maintaining its natural properties. Pure PS membranes and PS/NCC composite membranes were prepared using a Loeb–Sourirajan (L–S) phase inversion process. In this paper, the effect of NCC content, PS content, and additive content on permeability and morphology of composite membranes was studied. The surface and cross-section morphologies of the composite membranes were characterized by scanning electron microscopy (SEM). Besides, the pure water flux, Bovine serum albumin (BSA) rejection ratio, porosity, and mean pore size of composite membranes were also investigated.

2. Methods

2.1. Raw materials

The PS was purchased from China. Cellulose pulp was provided by Shandong Huatai Paper Mill (Shandong, China). BSA was purchased from Beijing Aoboxing Biological Technology Co., Ltd (Beijing, China). H_2SO_4 (95–98 wt%) and N,N-dimethylacetamide (DMAc) were purchased from Beijing Chemical Plant (Beijing, China). Polyethylene glycol 1000 (PEG 1000) was purchased from Beijing Chemical Reagent Company (Beijing, China).

2.2. NCC preparation

Cellulose pulp was immersed into H_2SO_4 (15 wt%) solution and reacted at 85°C by mixing thoroughly using an electric blender for 4 h. At the end of the reaction, the pH value of the solution was regulated until it was neutral using deionized water. After sieving and drying, the solids were submerged into DMAc and were homogenized with a high-pressure homogenizer (GEA Niro Soavi, Italy) [16]. Subsequently, a colloidal suspension of NCC was obtained which was then diluted to various concentrations of: 0, 0.1, 0.3, 0.5, 0.7, 0.9, and 1.1 wt%, in order to investigate the effect of the NCC on the composite membrane performance.

2.3. Membrane preparation

Composite membranes were prepared by a L–S phase inversion process. A quantity of PS and additives were dissolved in the NCC colloidal suspension (prepared in different concentrations). The casting solution was obtained by swaying at 50°C in the table concentrator (constant-temperature table concentrator, SHK-99-II, Beijing North TZ-Biotech Develop Co., China) for 24 h. After being vacuum degassed (with a vacuum degree of −0.1 MPa), an appropriate amount of the solution was dispersed uniformly on a glass plate in the ambient atmosphere. After being exposed in the air for 10 s, the glass plate was immersed into the water bath at room temperature. After complete coagulating and washing, the membranes were ready for characterization.

The compositions of casting solutions are listed in Tables 1–3.

Table 1
Compositions of dope solutions which added different NCC content

Code	Compositions of dope solutions (wt%)			
	PSF	NCC	DMAc	PEG 1000
A1	18	0	79.0	3
A2	18	0.1	78.9	3
A3	18	0.3	78.7	3
A4	18	0.5	78.5	3
A5	18	0.7	78.3	3
A6	18	0.9	78.1	3
A7	18	1.1	77.9	3

Table 2
Compositions of dope solutions which added different PS content

Code	Compositions of dope solutions (wt%)			
	PS	NCC	DMAc	PEG 1000
B1	12	0.3	84.7	3
B2	14	0.3	82.7	3
B3	16	0.3	80.7	3
B4	18	0.3	78.7	3
B5	20	0.3	76.7	3
B6	22	0.3	74.7	3
B7	24	0.3	72.7	3

Table 3
Compositions of dope solutions which added different PEG 1000 content

Code	Compositions of dope solutions (wt%)			
	PS	NCC	DMAc	PEG 1000
C1	18	0.3	81.7	0
C2	18	0.3	81.2	0.5
C3	18	0.3	80.7	1
C4	18	0.3	79.7	2
C5	18	0.3	78.7	3
C6	18	0.3	77.7	4
C7	18	0.3	76.7	5

2.4. Membrane characterization

2.4.1. Pure water flux, BSA solution flux, and rejection ratio

The pure water flux was tested according to the method described by Zhang et al. [26]. The volume of filtered water V (m^3) was obtained in some portions of the membrane with a working pressure of 0.1 MPa and a working time [t (h)]. Next, the pure water flux [J_w (L/(m^2 h))] was calculated with Eq. (1):

$$J_w = \frac{V}{At} \tag{1}$$

where V is the volume of filtered water (m^3), A is the membrane area (m^2), and t is the working time (h).

The BSA solution (1 g/L) flux was tested according to the method described by Zhang et al. [26]. The volume of filtered water V_b (m^3) was obtained in some portions of the membrane with a working pressure of 0.1 MPa and a working time [t (h)]. Next, the BSA solution flux [J_b (L/(m^2 h))] was calculated with Eq. (2):

$$J_b = \frac{V_b}{At_b} \tag{2}$$

where V_b is the volume of filtered water (m^3), A is the membrane area (m^2), and t_b is the working time (h).

The rejection ratio of the BSA solution (1 g/L) was tested under a working pressure of 0.1 MPa, and the absorbance of the filtered solution was measured at 280 nm with a UV-1801 ultraviolet–visible spectrophotometer (Third Analysis Apparatus Co., Shanghai, China) [26]. The rejection ratio was calculated with Eq. (3):

$$R = (1 - A_f/A_i) \times 100\% \tag{3}$$

where R is the rejection ratio (%) and A_f and A_i are the absorbance of the filtered and initial solutions, respectively.

2.4.2. Porosity and mean pore size

The porosity and mean pore size of the membranes were tested according to the method proposed by Zhang et al. [26]. The membrane, whose area was already known, was weighed in the hygroscopic state and then subsequently dried in an oven. The porosity [P_r (%)] and mean pore size [r (m)] of the membrane were calculated with Eqs. (4) and (5):

$$P_r = (W_w - W_d)/(d_w A_m L_m) \tag{4}$$

where W_w and W_d are the weight of the wet and dry membrane (g), respectively. d_w is the water density (g/cm^3), and A_m and L_m are the membrane area (cm^2) and thickness (cm), respectively.

$$r = [8 \times (2.9 - 1.75P_r) \cdot \eta LF/3,600\ P_r \Delta P]^{1/2} \tag{5}$$

where η is the viscosity of water (Pa s), L is the membrane thickness (m), F is the pure water flux (L/(m^2 h)), and ΔP is the working pressure (Pa).

The membrane thickness is measured by micrometer. Every membrane is divided into three equal regions. We select three points at random on each of three regions and measure the thickness of all nine points by micrometer. Then the measurements of membrane thickness are averaged. The measuring accuracy of micrometer is 0.01 mm.

2.4.3. Scanning electron microscopy

The composite membranes and pure PS membranes were broken in nitrogen liquid, so that the fractured cross-sections and the bottom surface of the membranes can be observed with SEM (S-3000n, Hitachi, Japan) after being sprayed with gold [27].

2.4.4. Scanning probe microscopy

The composite membrane which stored in dry condition was cut into the square shape with a side length of 5 cm. Then the composite membrane was characterized using a scanning probe microscope (9600n, Shimadzu, Japan). Images were collected using a phase mode with a constant force [28].

2.4.5. Antifouling performance

Firstly, the initial pure water flux of membrane [J_i (L/(m²h))] was measured before the UF process. Secondly, BSA solution (1 g/L) was processed by the UF membrane for 1 h. Then the membrane was cleaned by deionized water for 1 h. After membrane cleaning step, the recovery pure water flux of membrane [J_r (L/(m²h))] was measured.

The pure water flux attenuation coefficient [M (%)] was calculated with Eq. (6):

$$M = (J_i - J_r)/J_i \times 100\% \tag{6}$$

where M is pure water flux attenuation coefficient (%), J_i is the initial pure water flux of membrane (L/(m²h)), and J_r is the recovery pure water flux of membrane (L/(m²h)).

3. Results and discussion

3.1. Permeability and BSA retention performances of composite membrane

3.1.1. The effect of NCC contents on composite membrane permeability and BSA retention performance

The parameters of composite membranes preparation are listed as follows. The content of PS was 18 wt%. PEG 1000 acted as the additive and its contents was 3 wt%. The solvent was DMAc.

Deionized water acted as the coagulation bath, which was maintained at a temperature of 30°C. NCC concentration was set to 0, 0.1, 0.3, 0.5, 0.7, 0.9, and 1.1 wt %, respectively.

The data of the pure water flux of different membranes are depicted in Fig. 1. As shown in Fig. 1, the pure water flux of composite membrane increases with the increase of NCC concentration. When the NCC content ranges from 0 to 0.3 wt%, the pure water flux increases remarkably, when NCC content ranges from 0.3 to 0.7 wt%, the water flux has no obvious change, when NCC content continues to increase, which ranges from 0.7 to 1.1 wt%, the water flux increases significantly. When NCC content increases from 0 to 0.3 wt%, the pure water flux increases from 175.6 to 343.2 L/(m²h). NCC is a kind of material with nanometer scale. It possesses a huge specific surface area. Therefore, lots of hydroxyl groups are exposed at surface of NCC. Owing to the strong hydrophilicity of NCC, the hydrophilicity of composite membrane can be improved. During the phase inversion process, instantaneous demixing process can be speeded up by the existence of NCC. The membrane with high porosity and loosened structure can be formed. As a result, the pure water flux increases with the increase of NCC content at some extent.

The BSA rejection ratio results of different membranes are listed in Fig. 1. As shown in Fig. 1, the BSA rejection ratio does not decrease significantly with the increase of NCC content. When the NCC content increased from 0 to 0.7 wt%, the BSA rejection ratio decreased from 97.8 to 96.2%. The results of BSA rejection ratio all remain above 96%. It is indicated that
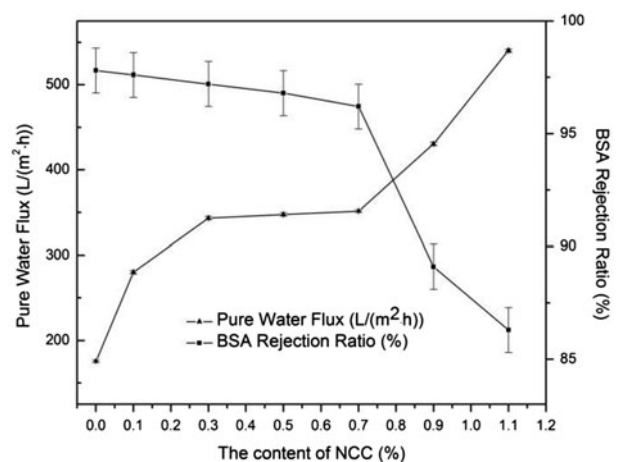

Fig. 1. Effect of NCC contents on the pure water flux and BSA rejection ratio of the composite membrane (NCC contents include 0, 0.1, 0.3, 0.5, 0.7, 0.9, 1.1 wt%, PS content is 18 wt%, DMAc content include 79.0, 78.9, 78.7, 78.5, 78.3, 78.1, 77.9 wt%, PEG 1000 content is 3 wt%).

the increase of NCC has little impact on the BSA rejection performance of composite membrane at some extent. When the content of NCC is more than 0.7 wt%, the value of BSA rejection ratio continues to decline, which is less than 90%. This is because high concentration of NCC causes the occurrence of agglomeration, which leads to the pore defects of membrane. Therefore, the BSA rejection performance of composite membrane is declined when adding excessive content of NCC.

After being processed by high-pressured homogenizer, the size of cellulose turns into nanometer scale. Therefore, the surface area increases sharply. So more hydroxyl groups of cellulose are exposed, surface energy of NCC is increased significantly. Owing to the strong hydrophilicity of NCC, during the phase inversion process, NCC in casting solution can absorb more water molecules, the rate of inter diffusion between precipitant (water) and solvent can be accelerated by the existence of NCC. Thus, the instantaneous demixing process can be speeded up and the dense layer with loosened structure is formed. With the increase of diffusion rate of precipitant (water) entering into casting solutions, the formation of the new nuclei in polymer-poor phase can be formed easily and the growth of new nuclei are promoted. As a result, the loosened sponge-like pore structure in dense layer and larger sized finger-like pore structure in support layer are formed. Because there are large amount of hydroxyl groups at surface of NCC, the existence of NCC in composite membrane can reduce the hydrophobic molecules adsorption. As a result, the permeability of composite membrane can be improved by adding proper amount of NCC. However, the effect of NCC on improving membrane performance should be based on good compatibility between NCC and PS. Owing to its small size and strong hydrophilicity, some of NCC might flow out with water during the process of inter diffusion between precipitant (water) and solvent. Therefore, when the NCC concentration ranges from 0.3 to 0.7 wt%, the pure water flux has no significant change. When the content of NCC is larger than 0.7 wt%, the interaction between NCC molecules is increased, which leads to agglomeration phenomenon. Therefore, more pore defects can be observed when adding over dose of NCC, so the pure water flux went up remarkably accompanied with significant decline of the BSA rejection ratio.

3.1.2. The effect of PS contents on composite membrane permeability and BSA retention performance

The parameters of composite membranes preparation are listed as follows. NCC content was 0.3 wt%.

PEG 1000 acted as the additive and its concentration was 3 wt%. The solvent was DMAc. Deionized water acted as the coagulation bath, which was maintained at a temperature of 30°C. Different content of PS (12, 14, 16, 18, 20, 22, 24 wt%) were added to the casting solutions, respectively.

The effects of PS contents on pure water flux and BSA rejection ratio of the composite membrane are depicted in Fig. 2. As can be seen from Fig. 2, with the increase of PS concentration, the pure water flux of composite membrane declines significantly and the BSA rejection ratio of the composite membrane increases remarkably. When the PS concentration increases from 12 to 24 wt%, the pure water flux decreases from 417.2 to 269.8 L/(m^{2}h), the BSA rejection ratio increases from 77.8 to 99.0%.

PS, as the main polymer in casting solution, is a basis of the realization of composite membrane performances. Therefore, most of membrane performances are depended on the factor of PS concentration. When PS concentration is low, the viscosity of casting solution is also low. During the phase inversion process, a loosened dense layer is formed in top surface of membrane, which plays a weak role on hindering precipitant to enter into membrane. As a result, precipitant (water molecules) can easily enter into membrane surface and promotes the formation of new nuclei of polymer-poor phase; large pore structure is finally formed. Thus, composite membrane with low PS concentration has good permeability but low BSA rejection rate.
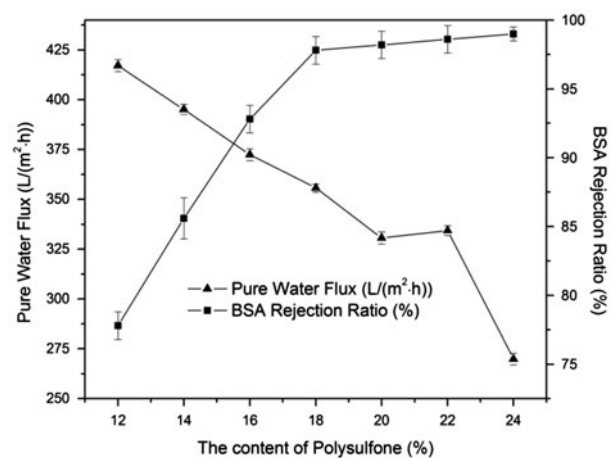

Fig. 2. Effect of PS contents on the pure water flux and BSA rejection ratio of the composite membrane (PS contents include 12, 14, 16, 18, 20, 22, 24, NCC content is 0.3 wt%, DMAc contents include 84.7, 82.7, 80.7, 78.7, 76.7, 74.7, 72.7 wt%, PEG 1000 content is 3 wt%).

However, with the increase of PS concentration, the viscosity of casting solutions increases. After the phase inversion process, the formed network structure of polymer is dense and stable. As a result, the size of pores that distributes on the top surface declines remarkably, which prevent the phase inversion process from happening rapidly. Moreover, owing to the increase of polymer content in casting solution, PEG 1000, which acts as additive, disperses as small micelle and pore size of finger-like pores becomes small, the connectivity of finger-like pores in support layer become poor. For the above analysis, with the increase of PS content, the pure water flux of composite membranes declines remarkably and the BSA rejection ratio increases significantly. In view of the data of BSA rejection ratio and the difficulty of membrane preparation when PS concentration is high, 18 wt% content of PS is selected.

3.1.3. The effects of PEG 1000 contents on composite mem-brane permeability and BSA retention performance

The parameters of composite membranes preparation are listed as follows. The content of PS was 18 wt%. NCC concentration was 0.3 wt%. The solvent was DMAc. Deionized water acted as the coagulation bath, which was maintained at a temperature of 30°C. PEG 1000 acted as the additive and different contents of PEG 1000 (0, 0.5, 1, 2, 3, 4, 5 wt%) were added to the casting solutions, respectively.

The effects of PEG 1000 contents on the pure water flux and BSA rejection ratio of the composite membrane are shown in Fig. 3. As depicted in Fig. 3, when PEG 1000 contents increased from 0 to 3 wt%, a remarkable increasing variation trend could be observed from the data of the pure water flux. When the content of PEG 1000 is 3 wt%, the pure water flux reaches the peak value, which is 367.8 L/(m^{2}h) compares to 221.9 L/(m^{2}h) of pure PS membrane. It is indicated that the permeability of composite membrane can be improved by increasing the PEG 1000 content at some extent. When the PEG 1000 contents is more than 3 wt%, no significant change can be seen from the pure water flux data. In addition, with the increase of PEG 1000 contents, a little decline of the BSA rejection ratio can be observed. When PEG 1000 contents increases from 0 to 5 wt%, the BSA rejection ratio decreases from 99.5 to 97.3%. It is indicated that the PEG 1000 contents has effect on BSA retention performance.

PEG 1000, as a kind of additive with good hydrophilicity, is swelling agent of polymer, which affects the dissolving ability of DMAc solvent and facilitates the formation of porous polymer network and micelles
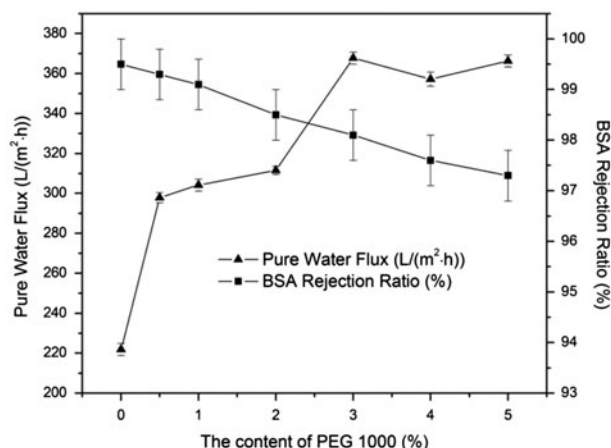

Fig. 3. Effect of PEG 1000 contents on the pure water flux and BSA rejection ratio of the composite membrane (PEG 1000 contents include 0, 0.5, 1, 2, 3, 4, 5 wt%, NCC content is 0.3 wt%, PS content is 18 wt%, DMAc contents include 81.7, 81.2, 80.7, 79.7, 78.7, 77.7, 76.7 wt%).

aggregation. After phase inversion process, PEG 1000 can dissolve in precipitant (water). Owing to the hydrophilicity of PEG 1000, during the phase inversion process, the inter diffusion exchange between solvent and precipitant (water) can be promoted by PEG 1000. According to pore forming mechanism, the increase of exchange rate between solvent and precipitant (water) can lead to easily formation of polymer-poor phase nuclei and can facilitate the formation of finger-like pores. This viewpoint can also be proved by SEM images. Fig. 10 shows the SEM images of top surface and cross-section of composite membrane with different PEG 1000 content. As shown in Fig. 10, when the PEG 1000 content is 0 wt% (Fig. 10(A1)), the size of finger-like pores are relatively short and the number of finger-like pores is low. With the increase of the PEG 1000 content, the size of finger-like pores becomes longer and the number of finger-like pores increases (Fig. 10(B1, C1, and D1)). Different content of PEG 1000 can make changes on the size and proportion of pores such as pores distributes on membrane top surface and pores formed by liquid–liquid demixing. Different content of PEG 1000 can influence the pore size and pore distribution and thus influences the membrane performance. Moreover, with the increase of PEG 1000 contents, the interaction between polymers is weakened and entanglement points are decreased. The polymer structure in casting solution becomes more loosened. During the phase inversion process, owing to the existence of PEG 1000, the rate of inter diffusion between solvent and precipitant (water) is speeded up, the solidification rate is

accelerated, loosened, and larger network pore structure is formed, which makes the structure of membrane performance layer loosened and uniform. As depicted in Fig. 10, when PEG 1000 content is 0 wt% (Fig. 10(A2)), few pores can be observed on the top surface of membrane, when the PEG 1000 content increases (Fig. 10(B2, C2, and D2)), the number of pores distributed on the top surface of membrane is increased. With the increase of PEG 1000 content, the finger-like pores are distributed uniformly (Fig. 10(B1, C1, and D1)) and the connectivity of those finger-like pores are better than that of the membrane without adding PEG 1000 content (Fig. 10(A1)). Consequently, with the increase of PEG 1000, the permeability of composite membrane is increased. Due to the little effect of PEG 1000 on increasing the pore sizes of membrane dense layer, no obvious change can be found in BSA rejection ratio. When the content of PEG 1000 is more than 3 wt%, the dispersion of PEG 1000 is limited by the main polymer (PS) in casting solution and the inter diffusion between solvent and precipitant (water) tend to saturation, the effect of PEG 1000 is not remarkable. So the permeability of membrane has no significant change when PEG 1000 contents is more than 3 wt%. From experimental results and the above analysis, 3 wt% is selected as the proper content of PEG 1000.

3.2. Characterizations of composite membrane pore structure

3.2.1. Effect of NCC concentration on pore structure of composite membrane

The parameters of composite membranes preparation are listed as follows. The concentration of PS was 18 wt%. PEG 1000 acted as the additive with a concentration of 3 wt%. The solvent was DMAc. Deionized water acted as the coagulation bath, which was maintained at a temperature of 30°C. NCC concentration was set to 0, 0.1, 0.3, 0.5, 0.7, 0.9, 1.1 wt%, respectively.

The effect of the NCC content on the porosity and mean pore size is listed in Fig. 4. Both porosity and mean pore size of membranes increases with the increase of NCC concentration. When NCC concentration increases from 0 to 1.1 wt%, the porosity and mean pore size of the composite membranes grows from 40.5 to 79.2% and from 33.6 to 52.4 nm, respectively.

Double diffusion equilibrium in phase inversion process cannot maintain with the existence of NCC due to its huge specific surface area and a large number of hydroxyl groups on its surface, which
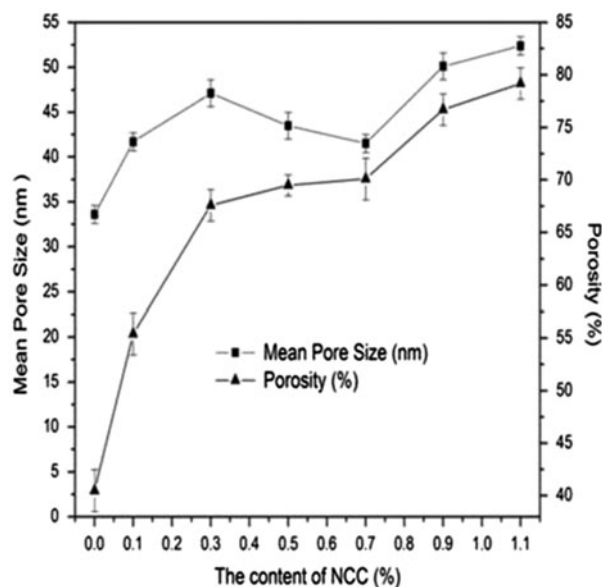

Fig. 4. Effects of the NCC contents on the porosity and mean pore size of the composite membrane. (NCC contents include 0, 0.1, 0.3, 0.5, 0.7, 0.9, 1.1 wt%, PS content is 18 wt%, DMAc content include 79.0, 78.9, 78.7, 78.5, 78.3, 78.1, 77.9 wt%, PEG 1000 content is 3 wt%).

means NCC is strongly hydrophilic. Due to its hydrophilicity, more water molecules could be adsorbed by NCC, forming a colloidal solution in the phase inversion process. Therefore, during the membrane formation process, the diffusion between gels (water) and solvent (DMAc) could speed up with the existence of NCC, which could promote the formation of new nuclei in polymer-poor phase. The pore structure with good connectivity could be easily formed with the promoted polymer-poor phase. In conclusion, the existence of NCC could be good for the formation of membranes with high porosity and mean pore size.

SEM images of cross-sections and top surface of membranes with different concentrations of NCC are given in Fig. 5. Typical asymmetric structures, composed of sponge-like dense layer and finger-like microporous support layer, can be observed in all of SEM images of the cross-section. In addition, with the increase of NCC concentration, the finger-like pores become longer and wider, which is good for its connectivity and results in the improvement of the membrane permeability. However, when the concentration of NCC is over 0.7%, the structure of membrane pores becomes irregular with larger void cavities, weakening the BSA retention performance of the membrane.

Those trends showed in SEM images might be explained as follows. Cellulose will change into small NCC after homogenization. Such small dimension
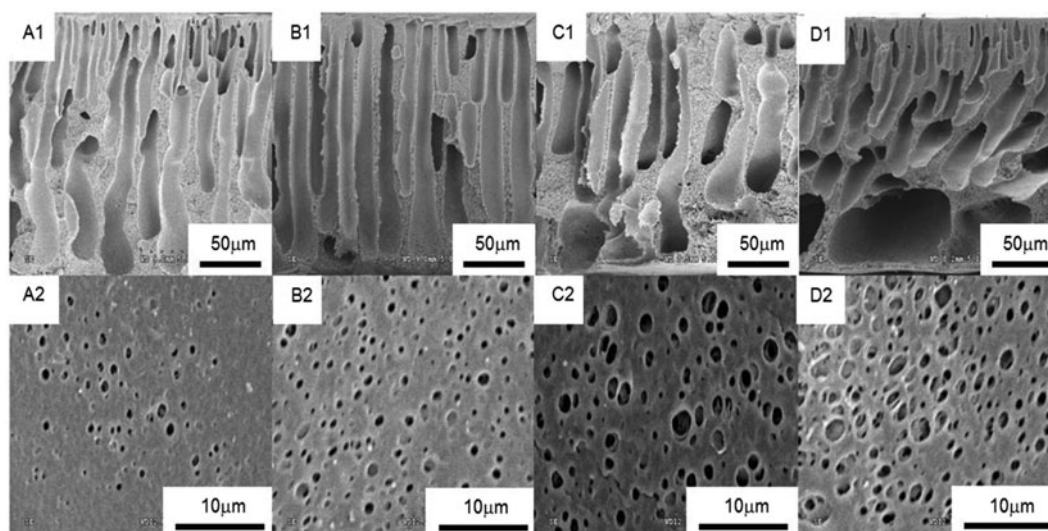
Fig. 5. SEM images of the cross-sections (A1, B1, C1, D1) and top surfaces (A2, B2, C2, D2) of the composite membranes with different NCC contents: (A1, A2) 0 wt%; (B1, B2) 0.3 wt%; (C1, C2) 0.7 wt%; (D1, D2) 1.1 wt%.

NCC will have huge specific surface area, which makes more hydroxyl groups exposed to the surface of NCC. With a good moisture-adsorbing capability, NCC could therefore adsorb more moisture to form a colloidal solution. Due to the good hydrophilicity of NCC, the diffusion rate which water flows into casting solution could speed up in the phase inversion process, which is beneficial to the formation and growth of new nuclei in polymer-poor phase. The condition for new nuclei continuously growth is described as follows. Before the curing of polymer-rich phase, the solution around the polymer-poor phase could continue to provide solvent to polymer-poor phase, and also due to the diffusion flow, the columnar-like and finger-like pore structure can be formed from the top surface to the bottom surface of the membrane. During the phase inversion process, the diffusion rate of solvent diffusing into precipitant (water) is much higher than the diffusion rate of precipitant (water) immersing into the casting solution, which leads to the formation of a loosened porous layer. The connectivity between membrane pores could be improved by this kind of sponge-like structure in membrane. However, the agglomeration effect, which could block pores or cause membrane defects in the phase inversion process, could be caused by adding excessive amount of NCC in the casting solutions. As a result, the membrane pore structure becomes irregular with large cavities.

The SPM images of the surface of pure PS membrane and composite membrane were depicted in Fig. 6. As can be seen from Fig. 6, NCC is distributed at the composite membrane bottom surface as individual and the PS NCC blend system shows sea/island morphology. PS acts as continuous phase and NCC acts as dispersed phase. As shown in the partially enlarged image of composite membrane (Fig. 6(C)), a complete NCC appears in rod shaped and its length and width are about 200 and 30 nm, respectively. Due to the good barrier action of PS molecules, the probability of NCC agglomeration is reduced and it is distributed uniformly in continuous phase through the phase inversion process, which improves the performance of the composite membranes.

3.2.2. Effect of PS concentration on pore structure of composite membrane

The parameters of the composite membranes preparation are listed as follows. NCC concentration was 0.3 wt%. PEG 1000 acted as the additive with a concentration of 3 wt%. The solvent was DMAc. Deionized water acted as the coagulation bath with a temperature maintained at 30°C. Different concentrations of PS (12, 14, 16, 18, 20, 22, 24 wt%) were added to the casting solutions, respectively.

The effects of the PS content on the porosity and mean pore size are shown in Fig. 7. As shown in Fig. 7, when the concentration of PS increases, the porosity of composite membranes experiences an initial fast increase followed by a decrease. When the
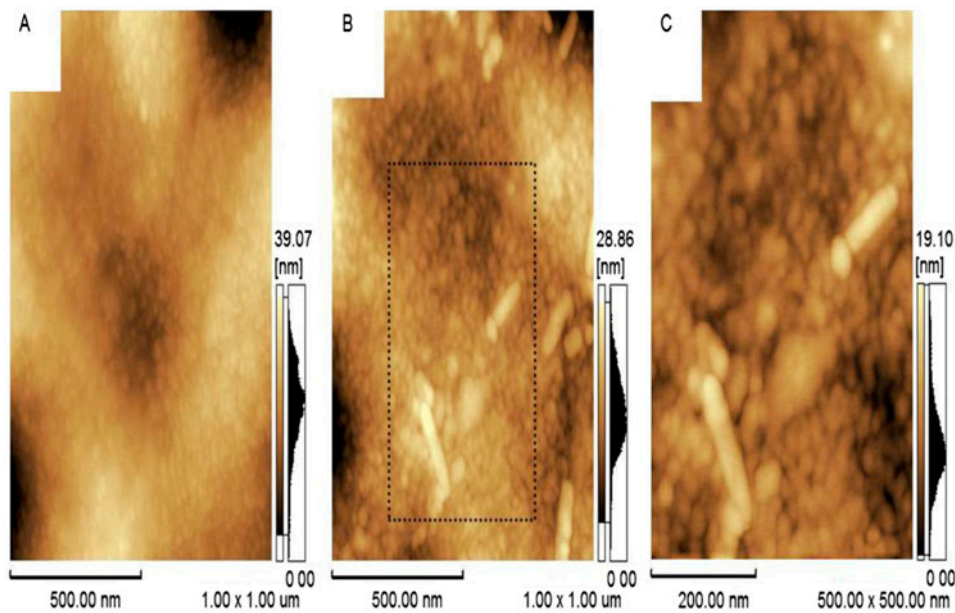
Fig. 6. SPM images of the surface of the composite membrane: (A) pure membrane, (B) composite membrane, and (C) partial enlargement of composite membrane.
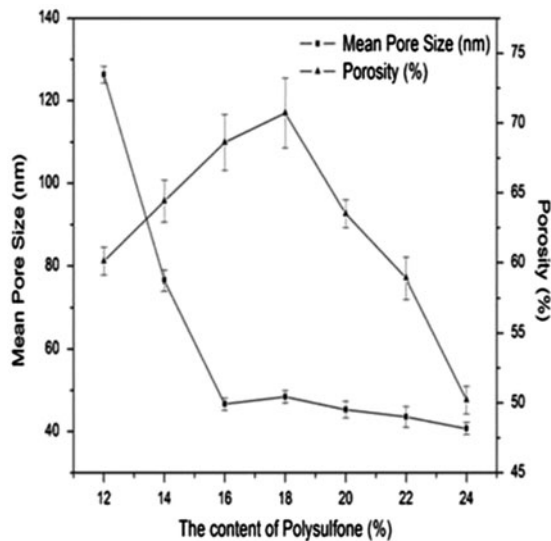

Fig. 7. Effects of the PS contents on the porosity and mean pore size of the composite membrane. (PS contents include 12, 14, 16, 18, 20, 22, 24 wt%).

Theoretically, if the concentration of PS in casting solution is low, when it is immersed into the coagulation, the concentration of polymer at initial phase separation point is also low. As a result, the polymer-poor phase accounts for larger proportion after phase separation process, forming membranes with high porosity and larger mean pore size.

The experimental results showed that the variation trend of mean pore size with increasing PS content matched the theory. It is remarkable that the porosity increased with the increasing concentration of PS when the concentration of PS was less than 18 wt%, which was opposite to theoretical expectation. This might be due to the fact that NCC played an important role in phase inversion process. When the concentration of PS was low, the formed dense layer was thin and the size of pores distributed at its surface was larger. Due to the excellent hydrophilicity of NCC, non-solvent could easily enter into the casting solution, forming the macroporous structure. Therefore, with the increase of PS content, the porosity of composite membrane increased at first, and then decreased.

Due to the increase of the concentration of PS, the viscosity of casting solution was enhanced, resulting in denser polymer network structure and the stronger interaction in molecular chains. The additive (PEG) dispersed in casting solution in the form of small micelles, reducing the pore sizes of both the network pores in the dense layer and finger-like pores in the

concentration of PS is 18 wt%, the porosity reaches its peak value of 70.7%. The mean pore size of composite membranes is decreased with the increasing concentration of PS. When the concentration of PS was over 18 wt%, the mean pore size maintains between 40 and 50 nm.

support layer. Moreover, during the process of phase separation, the increase of PS content would elongate the phase separation time and reduce the phase separation rate so that the structure of composite membrane became more compact.

It is the increasing PS concentration that resulted in thicker dense layer. The diffusion of precipitant (water) entering the casting solution was hindered by high concentration of PS. The formation and growth of finger-like pores were also restricted by high PS concentration. The decrease of both porosity and mean pore size of composite membrane was caused by the reduced number of finger-like pores in microporous support layer.

SEM images of cross-sections and top surface of membranes with different PS content are shown in Fig. 8. When the PS content is low (12 wt%), the pore structure of the support layer is irregular. Large finger-like pores and cavities could be observed and a number of large-sized pores (as large as 3 μm) are distributed on the top surface of composite membrane. When the PS content is increased to 18 wt%, a large number of small-sized pores are uniformly distributed on the top surface. The finger-like pores in the support layer are more regular and maintain good connectivity. When the PS content reaches 24 wt%, a small number of small-size pores spread on the top surface. The dense layer of composite membrane is thicker than that of the low content of PS composite membrane. The finger-like pores in the cross-section are short and thin form. Moreover, when the PS content is 24 wt%, few finger-like pores which could run through the top surface and the bottom surface could be observed in the cross-section SEM images. According to the above experimental observation and analysis, when PS content is 18 wt%, the porosity of composite membrane is the best compared to composite membranes containing different PS concentration.

3.2.3. Effect of PEG 1000 contents on pore structure of composite membrane

The parameters of composite membranes preparation are listed as follows. The concentration of PS was 18 wt% and the NCC concentration was 0.3 wt%. The solvent was DMAc. Deionized water was used as the coagulation bath, which was maintained at a temperature of 30°C. PEG 1000 was used as the additive and different concentrations of PEG 1000 (0, 0.5, 1, 2, 3, 4, 5) were added to the casting solutions, respectively.
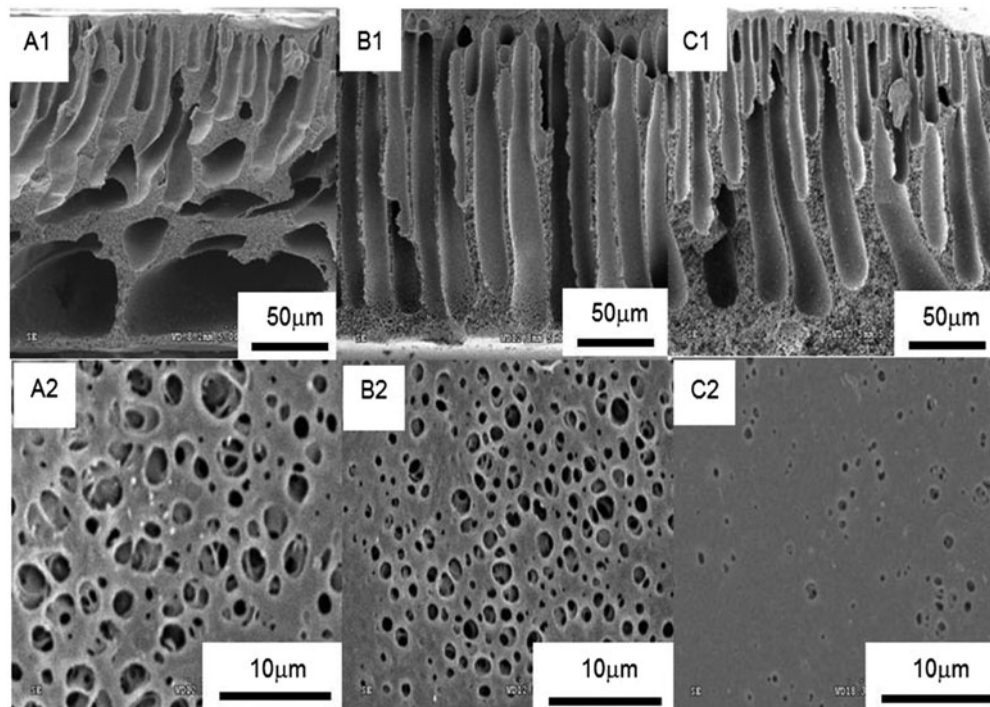

Fig. 8. SEM images of the cross-sections (A1, B1, C1) and top surfaces (A2, B2, C2) of the composite membranes with different PS concenrations: (A1, A2) 12 wt%; (B1, B2) 18 wt%; (C1, C2) 24 wt%.

The effects of different contents of PEG 1000 additives on the porosity and mean pore size are listed in Fig. 9. As depicted in Fig. 9, both of the porosity and mean pore size of composite membrane are increased with increasing PEG 1000 content. When the concentration was increased from 0 to 3 wt%, the porosity increased from 42.2 to 68.0%. When the concentration was above 3 wt%, there was no obvious change of the porosity. When the PEG 1000 concentration was increased from 0 to 5 wt%, the mean pore size increased from 30.1 to 57.4 nm.

The morphology of composite membranes with different PEG concentration is shown in Fig. 10. As depicted in Fig. 10, when the concentration of PEG 1000 was 0 wt%, narrow and short columnar pores existed in the cross-section images, and the sponge-like dense layer near the bottom surface was thick. There were fewer small-sized pores distributed on its top surface of composite membrane. With the increase of PEG 1000 concentration, finger-like pores gradually became longer and larger; the sponge-like dense layer gradually became thinner. When the concentration of PEG 1000 was more than 3 wt%, the finger-like pores could even extend to the region near the bottom surface. With the increase of the PEG 1000 concentration, more pores were distributed on the top surface of the membrane and the size of pores at the top surface gradually became larger.

PEG is a kind of additive with good hydrophilicity. It can be used as swelling agent or nonsolvent, which affects the dissolving capacity of DMAc and facilitates the formation of polymer network and micelles aggregation. Owing to its good hydrophilicity, during the phase inversion process, the diffusion exchange rate between solvent and precipitant could be promoted. According to the mechanism of pore formation, the nuclei of polymer-poor phase could be formed easily when the diffusion rate between solvent and precipitant speeded up, which facilitates the formation of finger-like large pores. Different concen-
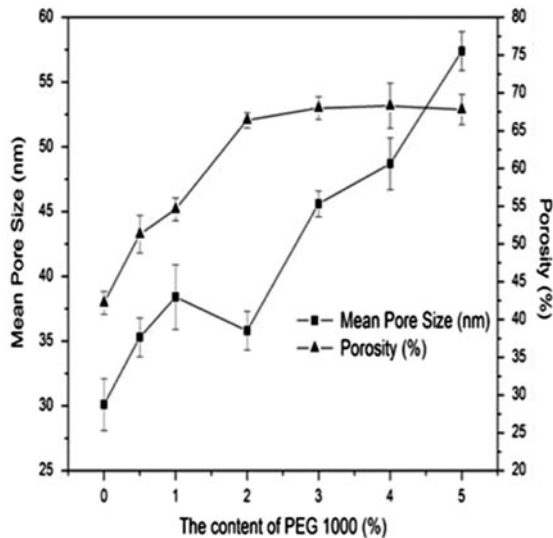

Fig. 9. Effects of the PEG 1000 contents on the porosity and mean pore size of the composite membrane. (PEG 1000 contents include 0, 0.5, 1, 2, 3, 4, 5 wt%).
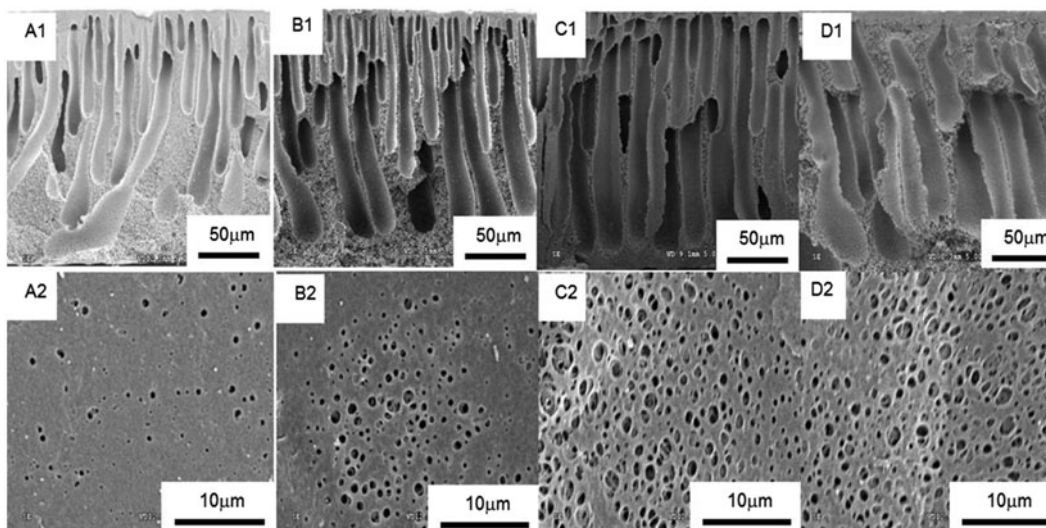

Fig. 10. SEM images of the cross-sections (A1, B1, C1, D1) and top surfaces (A2, B2, C2, D2) of the composite membranes with different PEG 1000 contents (A1, A2) 0 wt%; (B1, B2) 1 wt%; (C1, C2) 3 wt%; (D1, D2) 5 wt%.

tration of PEG 1000 had different effects on the size and quantity of network pores and micelles aggregation pores on the membrane surface. With the increase of PEG 1000 concentration, the interactions between polymer molecules were reduced as well as the entanglement points. Also, the structure of polymers in casting solution became more loosened. During the phase inversion process, the double diffusion rate between solvent and precipitant was accelerated, forming loosened finger-like pore structure and larger network pores. In conclusion, as the concentration of PEG 1000 increased, both of the porosity and mean pore size of composite membrane were increased, and the finger-like pores in cross-section gradually became longer and larger. The number of pores distributed on the top surface was increased and the pore size on top surface gradually became larger.

3.3. Permeability of BSA solution performance and antifouling performance of composite membrane

3.3.1. The effect of NCC contents on composite membrane permeability and antifouling performance

The initial pure water flux, BSA solution flux, and recovery of pure water flux of pure PS membrane and PS membranes blended with different content of NCC are shown in Fig. 11.

As shown in Fig. 11, the BSA solution flux of all the membranes is less than 50% of the corresponding pure water flux of the membranes. The BSA solution flux of pure PS membrane is lower than that of other
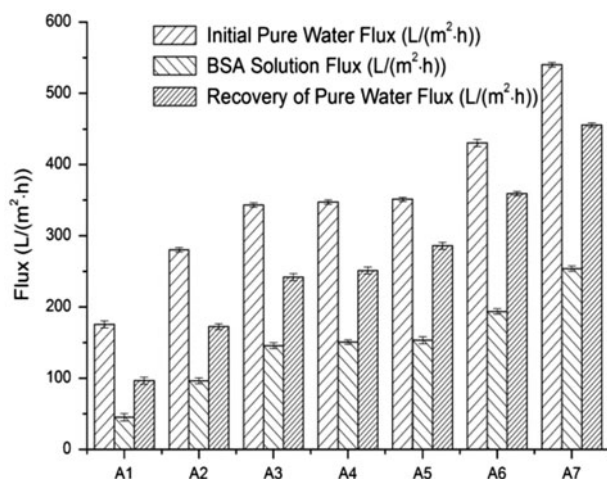

Fig. 11. The permeation fluxes of membranes blended with different content of NCC (NCC content: A1: 0 wt%, A2: 0.1 wt%, A3: 0.3 wt%, A4: 0.5 wt%, A5: 0.7 wt%, A6: 0.9 wt%, A7: 1.1 wt%).

membranes that adding NCC to casting solution, the BSA solution flux of membranes increases dramatically with the increase of the NCC contents, which increases from $45.2 \, L/(m^2 h)$ of pure PS membrane to $253.9 \, L/(m^2 h)$ of membrane blended with 1.1 wt% of NCC. This trend could be explained as follow. There are a large amount of hydroxyl groups exposed on the surface of NCC molecules. Therefore, NCC belongs to hydrophilic materials. The existence of NCC could improve the hydrophilic property of the membranes.

The pure water flux attenuation coefficient data of membrane blended with different content of NCC are shown in Table 4. Pure water flux attenuation coefficient data reflect the antifouling performance of membrane, the smaller the pure water flux attenuation coefficient, the better the antifouling performance. As depicted in Table 4, pure water flux attenuation coefficient value decreases with the increase of NCC content. So the antifouling performance of membrane is improved with the assistance of NCC.

3.3.2. The effect of PS contents on composite membrane permeability and antifouling performance

As shown in Fig. 12, the BSA solution flux of all the membranes is less than 50% of the corresponding pure water flux of the membranes. The BSA solution flux decreases with the increase of PS content. When PS content is 12 wt%, the BSA solution flux is $176.9 \, L/(m^2 h)$, when the PS content increases to 24 wt%, the BSA solution flux descends to 114.4 $L/(m^2 h)$. This is because PS is a kind of hydrophobic material. The PS content is higher, the hydrophilic property of membrane is worse.

The pure water flux attenuation coefficient data of membrane with different content of PS are shown in Table 5. As shown in Table 5, the pure water flux attenuation coefficient increases with the increase of PS content. As a result, lower content of PS is good for the antifouling performance of membrane.

Table 4
Pure water flux attenuation coefficient data of membrane blended with different content of NCC (NCC content: A1: 0 wt%, A2: 0.1 wt%, A3: 0.3 wt%, A4: 0.5 wt%, A5: 0.7 wt%, A6: 0.9 wt%, A7: 1.1 wt%)

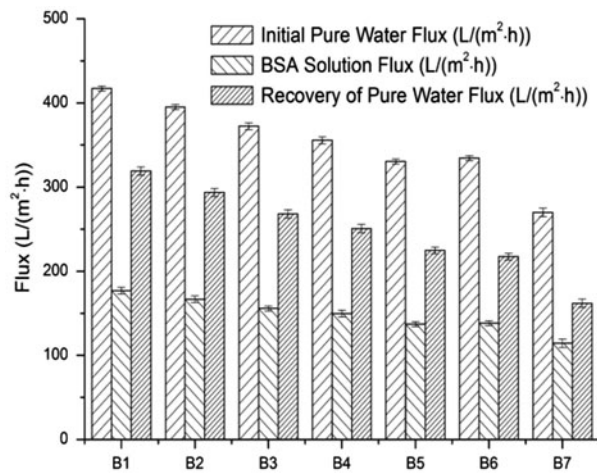| Membrane	A1	A2	A3	A4	A5	A6	A7
M (%)	45.0	38.4	29.5	27.7	18.6	16.5	15.7

Fig. 12. The permeation fluxes of membranes blended with different content of PS (PS content: B1: 12 wt%, B2: 14 wt%, B3: 16 wt%, B4: 18 wt%, B5: 20 wt%, B6: 22 wt%, B7: 24 wt%).

Table 5
The pure water flux attenuation coefficient data of membrane with different content of PS (PS content: B1: 12 wt%, B2: 14 wt%, B3: 16 wt%, B4: 18 wt%, B5: 20 wt%, B6: 22 wt%, B7: 24 wt%)

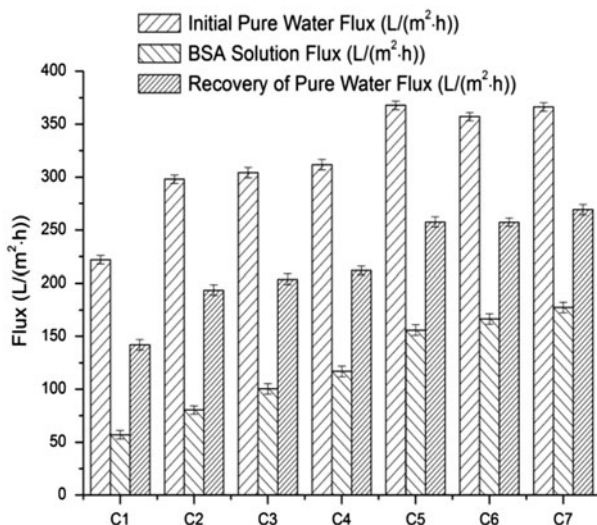| Membrane	B1	B2	B3	B4	B5	B6	B7
M (%)	23.5	25.7	28.0	29.5	32.0	34.9	40.0

Fig. 13. The permeation fluxes of membranes blended with different content of PEG 1000 (PEG 1000 content: C1: 0 wt%, C2: 0.5 wt%, C3: 1 wt%, C4: 2 wt%, C5: 3 wt%, C6: 4 wt%, C7: 5 wt%).

Table 6
The pure water flux attenuation coefficient data of membrane with different content of PEG 1000 (PEG 1000 content: C1: 0 wt%, C2: 0.5 wt%, C3: 1 wt%, C4: 2 wt%, C5: 3 wt%, C6: 4 wt%, C7: 5 wt%)

Membrane	C1	C2	C3	C4	C5	C6	C7
M (%)	36.0	35.0	33.0	31.9	30.0.	27.9	26.5

3.3.3. The effect of PEG 1000 contents on composite membrane permeability and antifouling performance

As shown in Fig. 13, the BSA solution flux of all the membranes is less than 50% of the corresponding pure water flux of the membranes. The BSA solution flux ascends with the increase of PEG 1000 content. When the PEG 1000 content is 0 wt%, the BSA solution flux is only 57.0 L/(m²h). When the PEG 1000 content is 5 wt%, the BSA solution flux reaches its peak value, 177.3 L/(m²h).

The pure water flux attenuation coefficient data of membrane with different content of PEG 1000 are shown in Table 6. As shown in Table 6, the pure water flux attenuation coefficient descends with the increase of PEG 1000 content. It is indicates that PEG 1000 has a positive effect on antifouling performance of membrane.

4. Conclusions

From the above experimental results and the analysis, the effect of NCC content, PS content, and additive content on permeability, morphology, porosity, and mean pore size of composite membranes was studied in this paper.

The addition of NCC accelerates the instantaneous demixing process. The pore size of membrane increases with the addition of NCC. With the increase of NCC contents, the permeability of composite membrane increases gradually. When the NCC content is 0.3 wt%, the pure water flux of composite membrane is far larger than that of the pure PS membrane, which is 343.2 L/(m²h) compared with 175.6 L/(m²h) of the pure PS membrane. When NCC content increased continually, the pure water flux increased insignificantly. When the NCC content ranges from 0 to 0.7 wt%, the BSA rejection ratio can maintain at a high level, which is more than 90%. When the NCC content is more than 0.7%, the agglomeration phenomenon of NCC leads to the defects of membrane pores, the permeability of composite membrane is improved, while the BSA rejection ratio declines remarkably.

With the increase of NCC content, the porosity and mean pore size of composite membrane would increase and the pore size of finger-like pores will become larger, improving the connectivity of finger-like pores. For the top surface of the membrane, the density of pores distributed on the top surface is increased and the pore size becomes large with the increase of NCC content. However, the agglomeration effect, which could block the pore or create membrane defects in phase inversion process, could be caused by adding excessive amount of NCC in the casting solutions. As a result, when the content of NCC is excessive, the membrane pore structure becomes irregular and it is accompanied with large cavities.

With the increase of PS content, the pure water flux of composite membrane decreases and the BSA rejection ratio increases. With the increase of PS content, the mean pore size of composite membrane decreases and the porosity of composite membranes will experience an increase at first, and then a decrease. When the concentration of PS is 18 wt%, the porosity reaches its peak value of 70.7%. Meanwhile, with the increase of PS concentration, the size of finger-like pores becomes short and thin, and both of the density and size of pores distributed on membrane top surface would decrease.

The permeability of composite membrane is improved remarkably by the addition of PEG 1000. When the content of PEG 1000 ranged from 0 to 3 wt%, the permeability increased with the increase of PEG 1000 content. When PEG 1000 content was more than 3 wt%, with the increase of PEG 1000 content, the permeability changed insignificantly. With the increase of PEG 1000 content, the BSA rejection ratio of composite membrane shows a trend of decline. However, the BSA rejection ratio can remain at a high level, which is more than 90%.

With the increase of PEG 1000 contents, the porosity and mean pore size of composite membrane are increased, the pore size of finger-like pores is increased, and a large number of pores are well distributed on the top surface of the composite membrane.

Acknowledgments

References

[1] M. Padaki, A.M. Isloor, P. Wanichapichart, Preparation and characterization of sulfonated polysulfone and N-phthloyl chitosan blend composite cation-exchange membrane for desalination, Desalination 298 (2012) 42–48.

[2] H.L. Bai, X. Wang, Y.T. Zhou, L.P. Zhang, Preparation and characterization of poly(vinylidene fluoride) composite membranes blended with nanocrystalline cellulose, Prog. Nat. Sci. Mater. Int. 22(3) (2012) 250–257.

[3] P. Qu, H.W. Tang, Y. Gao, L.P. Zhang, S.Q. Wang, Polyethersulfone composite membrane blended with cellulose fibrils, BioResources 5(4) (2010) 2323–2336.

[4] Z.F. Fan, Z. Wang, N. Sun, J.X. Wang, S.C. Wang, Performance improvement of polysulfone ultrafiltration membrane by blending with polyaniline nanofibers, J. Membr. Sci. 320 (2008) 363–371.

[5] I.C. Kim, J.G. Choi, T.M. Tak, Sulfonated polyethersulfone by heterogeneous method and its membrane performances, J. Appl. Polym. Sci. 74(8) (1999) 2046–2055.

[6] S.H. Choi, J.W. Chung, R.D. Priestley, Functionalization of polysulfone hollow fiber membranes with amphiphilic β-cyclodextrin and their applications for the removal of endocrine disrupting plasticizer, J. Membr. Sci. 409–410 (2012) 75–81.

[7] Z.F. Fan, Z. Wang, M.R. Duan, J.X. Wang, S.C. Wang, Preparation and characterization of polyaniline/polysulfone nanocomposite ultrafiltration membrane, J. Membr. Sci. 310 (2008) 402–408.

[8] B. Wang, B.W. Cheng, Y.F. Cui, Preparation of polysulfone hollow fiber affinity membrane modified with Mercapto and its recovery properties. I. Synthesis and preparation of hollow fiber matrix membrane, J. Appl. Polym. Sci. 100 (2006) 758–771.

[9] L. Yan, Y.S. Li, C.B. Xiang, Preparation of poly(vinylidene fluoride)(pvdf) ultrafiltration membrane modified by nano-sized alumina (Al$_2$O$_3$) and its antifouling research, Polymer 46 (2005) 7701–7706.

[10] G.P. Wu, S.Y. Gan, L.Z. Cui, Y.Y. Xu, Preparation and characterization of PES/TiO$_2$ composite membranes, Appl. Surf. Sci. 254 (2008) 7080–7086.

[11] Z.P. Fang, Y.Z. Xu, C.W. Xu, Modification mechanism of nanoparticles on polymers, J. Mater. Sci. Eng. 21(2) (2003) 279–282.

[12] P. He, A.C. Zhao, Nanometer composite technology and application in polymer modification, Acromolecule Aviso 2 (2001) 74–82.

[13] F. Liu, M.R. Moghareh Abed, K. Li, Preparation and characterization of poly(vinylidene fluoride) (PVDF) based ultrafiltration membranes using nano γ-Al$_2$O$_3$, J. Membr. Sci. 366 (2011) 97–103.

[14] E. Yuliwati, A.F. Ismail, Effect of additives concentration on the surface properties and performance of PVDF ultrafiltration membranes for refinery produced wastewater treatment, Desalination 273 (2011) 226–234.

[15] D. Klemm, D. Schumann, F. Kramer, N. Heßler, M. Hornung, H. Schmauder, S. Marsch, Nanocelluloses as innovative polymers in research and application, Adv. Polym. Sci. 205 (2006) 49–96.

[16] S. Li, Y. Gao, H.L. Bai, L.P. Zhang, P. Qu, L. Bai, Preperation and characteristics of polysulfone dialysis composite membranes modified with nanocrystalline cellulose, BioResources 6(2) (2011) 1670–1680.

[17] M. Henriksson, L.A. Berglund, Structure and properties of cellulose nanocomposite films containing melamine formaldehyde, J. Appl. Polym. Sci. 106(4) (2007) 2817–2824.

[18] S. Beck-Candanedo, M. Roman, D.G. Gray, Effect of reaction conditions on the properties and behavior of wood cellulose nanocrystal suspensions, Biomacro molecules 6(2) (2005) 1048–1054.

[19] F.W. Herrick, R.L. Casebier, J.K. Hamilton, K.R. Sandberg, Microfibrillated cellulose: Morphology and accessibility, J. Appl. Polym. Sci. 37(9) (1983) 797–813.

[20] K. Abe, S. Iwamoto, H. Yano, Obtaining cellulose nanofibers with a uniform width of 15 nm from wood, Biomacromolecules 8(10) (2007) 3276–3278.

[21] Q.Z. Cheng, S.Q. Wang, T.G. Rials, Poly(vinyl alcohol) nanocomposites reinforced with cellulose fibrils isolated by high intensity ultrasonication, Composites Part A 40 (2009) 218–224.

[22] A. Chakraborty, M. Sain, M. Kortschot, Cellulose microfibrils: A novel method of preparation using high shear refining and cryocrushing, Holzforschung 59(1) (2005) 102–107.

[23] J. Lu, P. Askeland, L.T. Drzal, Surface modification of microfibrillated cellulose for epoxy composite applications, Polymer 49(5) (2008) 1285–1296.

[24] R. Li, J. Fei, Y. Cai, Y. Li, J. Feng, J. Yao, Cellulose whiskers extracted from mulberry: A novel biomass production, Carbohydr. Polym. 76(1) (2009) 94–99.

[25] J. Ganster, H. Fink, Novel cellulose fibre reinforced thermoplastic materials, Cellulose 13(3) (2006) 271–280.

[26] L.P. Zhang, G.W. Chen, H.W. Tang, Q.Z. Cheng, S.Q. Wang, Preparation and characterization of composite membranes of polysulfone and microcrystalline cellulose, J. Appl. Polym. Sci. 112(1) (2009) 550–556.

[27] Q.Z. Cheng, S.Q. Wang, T.G. Rials, S.H. Lee, Physical and mechanical properties of polyvinyl alcohol and polypropylene composite materials reinforced with fibril aggregates isolated from regenerated cellulose fibers, Cellulose 14 (2007) 593–602.

[28] P. Qu, Y. Gao, G.F. Wu, L.P. Zhang, Nanocomposites of poly(lactic acid) reinforced with cellulose nanofibrils, Bioresources 5(3) (2010) 1811–1823.